Energy Conversion and Management 228 (2021) 113597

Contents lists available at ScienceDirect

Energy Conversion and Management

journal homepage: www.elsevier.com/locate/enconman

A residential community-level virtual power plant to balance variable renewable power generation in Sweden

Svante Monie *, Annica M. Nilsson, Joakim Widén, Magnus Åberg

Department of Engineering Sciences, Division of Civil Engineering and Built Environment, Built Environment Energy Systems Group (BEESG), Uppsala University, Uppsala, Sweden

ARTICLE INFO

Keywords:
Virtual power plant
Thermal energy storage
Power balancing
Power to heat
Variable renewable electricity
Combined heat and power

ABSTRACT

Power systems with large shares of variable renewable electricity generation, i.e., wind and solar power, require high flexibility in both power generation and demand. Heat pumps and combined heat and power units within district heating systems, and thermal storages have previously been studied for their potential to increase the flexibility of the energy system. When using these technologies for power balancing, they must be operated in a non-standard way with switched merit-order. This study hypothesizes that a residential area could form a local operated entity, i.e., a virtual power plant, that provides power-balancing services to a national power system. The hypothesis is tested with a case-study in Sweden where a combined heat and power unit, heat pumps, a local heat distribution system, and a thermal storage constitute the local entity. A simulation of the energy balances in the system, with optimization of storage size, was performed. The results show that all power surpluses in the system are consumed by the heat pumps. 43% of the annual and 21% of the electricity peak load are covered by the combined heat and power unit. It is concluded that an inter-seasonal thermal storage is crucial for the system's flexibility. Also, large electricity surpluses, if converted to heat and stored, limit the ability of the virtual power plant to utilize the combined heat and power unit for power balancing at a later stage. Despite this, a local virtual power plant can provide increased flexibility by offering power-balancing services to the power system.

1. Introduction

In December 2019, as a response to the United Nation's 2030 Agenda and the Paris Agreement [1], the European Commission announced a "European Green Deal" [2]. This deal contains explicit goals to decarbonize energy sectors and increase wind power production. This means that variable renewable electricity (VRE) generation, mainly from wind power, but to some extent also from photovoltaic (PV) systems, will likely increase in Europe in the future. VRE production is challenging because of its limited ability to instantly match the electricity demand. Mismatches between electricity production and electricity demand affect the stability of power distribution grids, and increase the risks of grid congestions [3]. Power grid reinforcements are a potential solution to this problem, but this is considered costly and time-consuming [4]. Therefore, with large shares of VRE generation the power production system must be able to both cover production deficits using additional power generation capacity and handle production surpluses. Several studies address the need for additional power generation capacity. For the Nordic power system, Olauson et al. [5] conclude that a 100% renewable electricity production, including a mix of VRE technologies, would need an additional power generation capacity in hydro or thermal power plants of 9–11 GW. Holttinen and Hirvonen [6] state that with a 10% share of VRE in the production mix, the demand on balancing power capacity will be in the range of 2–8% of installed wind power capacity. Hirth and Ziegenhagen [7] show in a literature review that the back-up capacity requirements, following an increased share of VRE, range from 2 to 20% of the installed VRE capacity.

In Sweden, the balancing power capacity is primarily provided through hydro power and condensing thermal power. The possibility to increase hydro power capacity is limited, mainly due to the fact that the water flow capacity in most rivers is already utilized for power generation. It is possible to increase the condensing thermal power generation capacity, but the technology suffers from low efficiency when based on renewable fuels (biomass or incinerable waste). The overall energy efficiency of thermal power generation is, however, significantly higher if the condensed heat is utilized, as in combined heat and power (CHP)

* Corresponding author at: Box 534, 751 21 Uppsala, Sweden.
E-mail addresses: svante.monie@angstrom.uu.se (S. Monie), annica.nilsson@angstrom.uu.se (A.M. Nilsson), joakim.widen@angstrom.uu.se (J. Widén), magnus.aberg@angstrom.uu.se (M. Åberg).

https://doi.org/10.1016/j.enconman.2020.113597
Received 11 May 2020; Received in revised form 23 October 2020; Accepted 24 October 2020
Available online 27 November 2020

plants. CHP production requires a user for produced heat, either through an industrial heat demand or by access to a district heating system (DHS). The fact that electricity and heat are co-produced when CHP is used for power balancing means that the size and variations of the heat demand limits the power generation. The possibility to cover VRE deficits using CHP production has been studied to some extent. For instance, Kubik et al. [8] show how CHP plants in Ireland can be operated to reduce curtailment of wind power. This was achieved partly at the expense of increased CO_2 emissions due to increased part-load operation of the plants. Furthermore, Hong et al. [9] show that CHP could play an important role in power balancing production in systems with high shares of VRE, but the results also showed that an increased operation flexibility of CHP plants is necessary to avoid excess electricity production. However, the possibility to use CHP plants to cover deficits in VRE production needs further investigations.

District heat production is not limited to CHP plants, but is flexible in the sense that heat can be produced in many ways. For example, large-scale heat pumps and/or electric boilers can be used to produce heat while consuming electricity, generally referred to as power-to-heat (P2H) production. P2H production in DHSs can handle surpluses in VRE production and can, thus, be considered a demand side management solution for large shares of VRE. P2H in DHSs has been investigated on national level for Germany by Böttger et al. [10] and for Sweden by Schweiger et al. [11]. Böttger et al. conclude that the theoretical potential for P2H in Germany is 32 GW_{el} but that the technical potential, due to limitation on both supply and demand sides, is 20 GW_{el} or less. Schweiger et al. find that for scenarios where VRE generation covers 54–64% of Sweden's annual electricity demand, P2H in current DHSs potentially can reduce surpluses in VRE generation by about 50%. Salpakari et al. [12] simulated how P2H in a DHS can significantly reduce surpluses in VRE generation on city level in Helsinki, Finland. The research, thus, suggest that P2H and CHP in DHSs have the potential to facilitate increased shares of VRE generation by reducing risks for adverse power grid instabilities. It is, in the light of this, important to note that the conditions for increasing the shares of VRE in Sweden are favorable since DHSs exist in nearly every Swedish city, often with CHP production. Also, DHSs in Sweden are, due to historically low electricity prices, in many cases equipped with large-scale heat pumps and/or electric boilers. These systems could play an important role in a future Swedish power generation system.

However, there are challenges. District heat demand in colder climates, as in Sweden, is constituted mainly of space heating in buildings. This means that the heat demand, which is the limiting factor for power production in CHP units as well as electricity use in P2H units, is higher in the winter than in the summer. Consequently, the potential to cover deficits and use surpluses in VRE production is significantly higher in the winter compared to the summer. This is unless heat can be stored for longer periods of time. Thermal energy storages (TES), most commonly water-filled ground pits, rock caverns or accumulator tanks can be used for levelling the heat supply in DHSs. This has been used previously, and is to some extent also currently used, but mostly for seasonal storage of heat produced by thermal solar panels. Studies have also investigated TESs in combination with CHP and/or P2H systems. For example, Rinne and Syri [13] show that for Finland, with a 24% share of VRE in the national production mix, the CHP electricity production can potentially increase by 15% when CHP is combined with TES. Hast et al. [41] find that a TES in a DHS with heat pumps, CHP, and heat-only boilers would be cost-effective for high shares of VRE. Dahl et al. [14] model, using linear programming, a fossil-free city-scale energy system with CHP, heat pumps, and TES. The results indicate that heat pumps combined with TES will supply most of the local heat demand. Both Dimoulkas et al. [15] and Schweiger et al. [11] imply that TESs can be used to help increase the shares of VRE in national power systems by using P2H. Lamaison et al. [16] used mixed integer linear programming to simulate a DHS with TES, P2H, and a heat-only biomass boiler. The study concludes that, for high shares of VRE, a long-term TES was required to reach a high share of renewables.

None of these studies, however, thoroughly investigate the use of the TES when the heat supplies from both CHP and heat pumps follow the production of VRE. The VRE variability, and thus the variability of the heat supply, makes it difficult to optimize the use of TESs. This means that even though TESs have been simulated, tested and used previously, they have not been investigated thoroughly for the purpose of storing heat from CHP and P2H that do not follow a regular heat supply pattern. Investigating this further is important, as these systems must be coordinated in order not to sub-optimize the operation of TESs.

Coordination of heat and electricity production units, often in combination with energy storages, to achieve, for example, power grid stability, is in the literature generally referred to as a virtual power plant (VPP). The study presented in this article considers a technical VPP, which is defined by VPP components that are within the same geographical region and physically connected [17]. Previous studies that have investigated DHSs as technical VPPs are, for example, Wille-Haussmann et al. [18] that performed an optimization of a VPP with five CHP units, heat only boilers, and a TES in a DHS. The results show that the optimal VPP-solution reduced the production costs with 10% compared to actual production data from the system as currently operated. Furthermore, in Sowa et al. [19], a DHS with P2H and TES was considered as a VPP used to reduce surplus VRE generation from wind power.

Combining CHP, P2H and TESs in DHSs as a VPP for power balancing requires operating these units in non-standard ways. CHP plants are usually operated to primarily supply local heat demands, and the co-produced electricity is a by-product that generates revenues to reduce heat production costs. When used to cover deficits in VRE production, the merit-order of heat and electricity produced in CHP plants is switched. The co-generated heat instead becomes the by-product of the generated electricity. Something similar happens for heat pumps and electric boilers. These units are generally used for heat production when electricity prices are low or as back-up production units. When heat pumps and electric boilers are used for P2H to reduce surpluses in VRE generation the produced heat is no longer the main product, but rather the by-product of consuming electricity. The size and flexibility of the heat demand will therefore be crucial for the performance of the VPP. The hypothesis of this study is that a residential area can form a local operated entity that provides power-balancing services to a national power system with large shares of VRE. The assumption is that established heat supply and heat storage systems are utilized, but operated in a novel fashion where power balancing takes priority over heat supply. The hypothesis is tested with a case-study where a single-family residential area in Sweden is the local entity and a Nordic power system with large shares of VRE is the receiver of the power balancing services. The idea can, however, be applied to any residential area, town, or even city that possess the technological infrastructure.

1.1. Aim and research questions

The overall aim of this study is to investigate to what extent a VPP based on established heat supply and heat storage technologies can contribute to VRE balancing, and what differences in system configuration are required as opposed to traditional operation. A typical Swedish single-family home residential area is used as a case study. A DHS with a CHP unit, heat pumps, and a TES is operated to reduce VRE surpluses and to cover VRE deficits for a future scenario with a high share of VRE in the national power generation system, as well as a significant amount of building applied photovoltaics (BAPV) within the residential area. The following research questions are answered:

1. To what extent can the local energy system contribute to reduce VRE power surpluses and cover deficits for high shares of local BAPV and VRE in the national power generation system?

2. How does the coordination of the production units, when used with a TES to reduce VRE deficits and surpluses, affect the dimensioning of the CHP and heat pump production capacities?
3. What is the overall efficiency of the TES when operated as a component of a VPP?

1.2. Scope and delimitations

This study has a technical approach and does not consider economic or policy aspects that might influence the system performance.

In this study some simplifications have been chosen. The local energy system is operated under conditions of perfect forecast. The local CHP have been assumed to have a fixed power-to-heat ratio. The impact of these simplifications on the results is addressed in the discussion.

The paper is structured as follows. In Section 2 the methods and materials used in the study are presented, including the case studied, setup of the VPP, deriving of the power balance demand, and algorithm decision strategy. In Section 3 the results from the simulations are presented. In Section 4 methods and the results are discussed, and finally conclusions are drawn in Section 5.

2. Method and materials

In Section 2.1 follows a description of the case studied to test the hypothesis Section 2.1, followed by a description of the components in the VPP in Section 2.2. In Section 2.3 is the power balancing demand that is used in the simulations presented and Section 2.4 gives a description of the decision strategy of the simulation's algorithm.

2.1. Residential area

The investigated residential area consists of 111 detached single-family houses built in the late 1960s. The area is located in a small community about 80 km north of Stockholm, Sweden. The area is of a common type of Swedish residential area with single-family buildings. Similar areas can be found all over the country and were built in the years 1965 to 1974, which was a period when a large share of the currently existing residential buildings in Sweden were built. Fig. 1 shows a map of the area with the properties, building footprints and streets.

Previously, the building energy efficiency potential in this specific

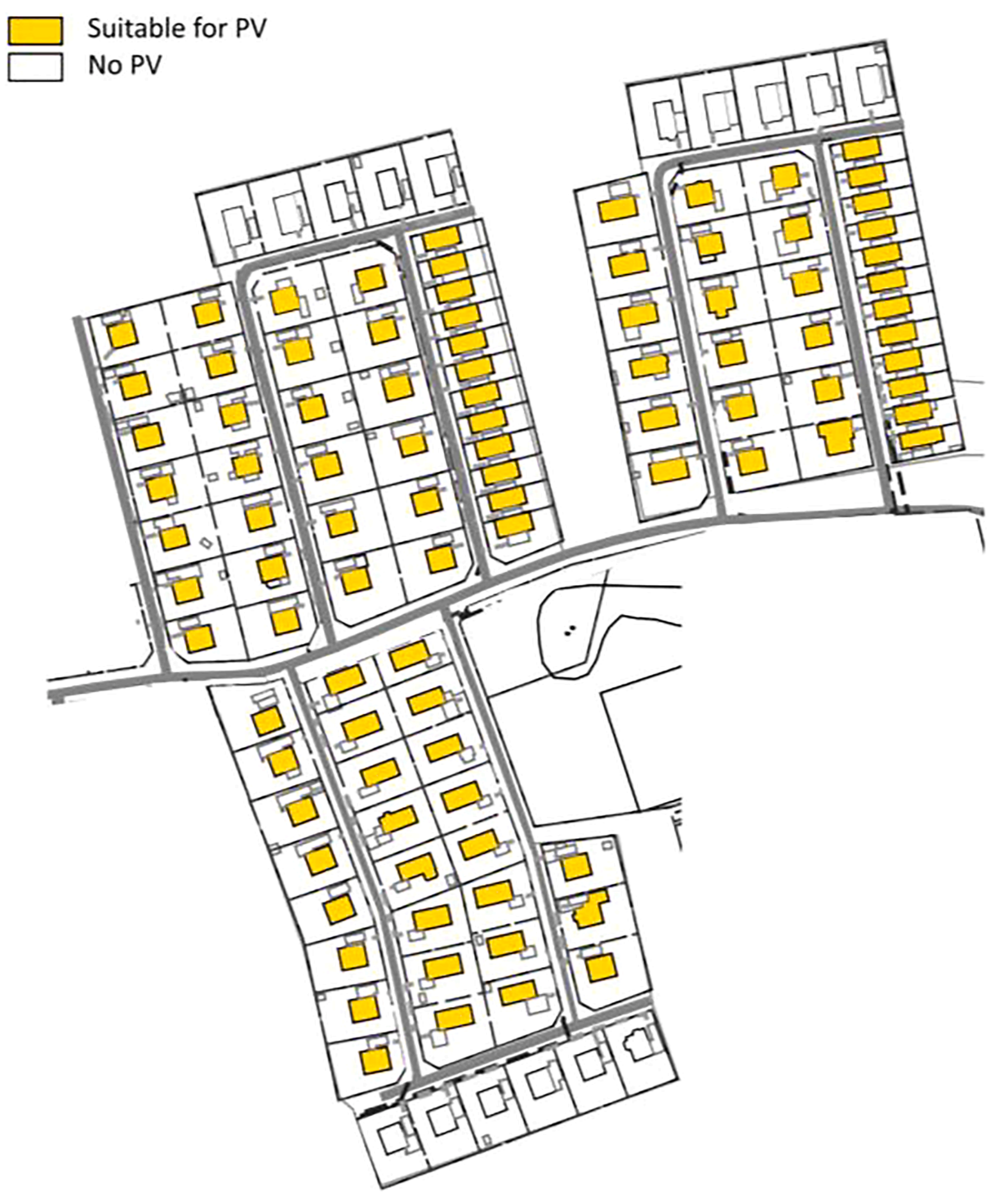

Fig. 1. Studied area with DHS and houses suitable for PV.

area was studied, as well as the CHP production possibilities with a traditional CHP production strategy, electricity demand due to home-charging of electric vehicles, and PV generation on the available roof-top areas. These results were presented in Åberg et al. [20], and the study presented in this paper is a continuation of that initial study. Some of the assumptions and calculations made and presented in Åberg et al. [20] are used here and considered as starting points for this study. The calculations from Åberg et al. [20] that are used are briefly described in the following.

The buildings are assumed to have undergone significant refurbishments and energy efficiency improvements. The energy balances of the buildings were simulated using the commercial software VIP-Energy (validated according to ASHRAE 140-2007 and EN 1526-2007), considering weather data, operational strategies, and material properties of the building envelopes, building shapes, and HVAC systems. The simulated specific energy use for heating and domestic hot water after refurbishments is 59 kWh/m^2 (the recommended energy use for new buildings in Sweden is 90 kWh/m^2).

The household electricity consumption was simulated using a stochastic Markov-chain model that generates stochastic household activity patterns where activities are associated with different power demands. Simulations were made on a minute-basis resolution and then averaged to hourly values. For detailed description of the model structure, calibration and validation, see Widén and Wäckelgård [21].

Simulations of power generation from BAPV were performed using meteorological data from 2014 and a method described in detail in Lingfors [22]. 95 of the 111 buildings were selected to have suitable south-facing roof orientation. These are marked in yellow in Fig. 1. Out of the total roof area on these 95 buildings, up to 25% of the available roof area was assumed to be covered with BAPV panels. 15% of the roof areas were assumed to be occupied by chimneys and ventilation ducts or shadowed from surrounding objects, and were therefore considered non-available. The BAPV simulation assumed to be varied from 0 to 150 kW$_p$ (where 150 kW$_p$ equals an installation of 25% of the available roof areas). Max installed BAPV corresponds to a penetration level of 27% where it has been assumed that each household that installs solar panels installs a "standard-sized" panel of 5 kW$_p$ (see Table 1). All buildings were assumed to be connected to a local DHS for which heat losses were calculated on an hourly basis for a full year.

2.2. The components and set-up of the virtual power plant

In this section the technologies of the simulated local virtual power plant are generally described, as well as how these are represented in this particular study. These technologies are the CHP production unit, the heat pumps, and the TES. Fig. 2 is a schematic picture of the system set-up with the different components and how these are connected. Components that are added in this study compared to Åberg et al. [20] are heat pumps and TES as well as the interaction with the upstream grid in terms of a VRE balancing signal from the national power grid.

2.2.1. Combined heat and power

The CHP unit in this study is assumed to be a biomass fueled Organic Rankine Cycle (ORC) unit with a thermal output of 400 kW$_{th}$. Traditionally a CHP unit is dimensioned to cover only part of the load, whereas the peak demand is to be supplied by a peak load unit (top-up) such as a heat only boiler [23]. In this way, the capacity factor or usage

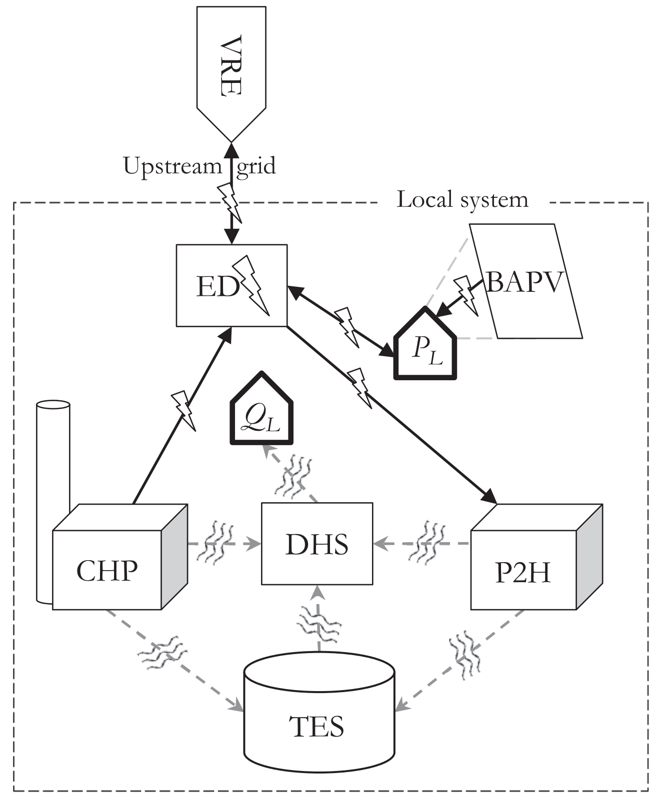

Fig. 2. Set-up of the studied system. ED is the local electric distribution, e.g. substation and power lines. Q_L, P_L, DHS, and BAPV are described in detail in Åberg et al. [20].

of the CHP unit is improved. This study attempts to use the TES for top-up supply. The electricity-to-heat output ratio was assumed to be constantly 0.2, which is a typical ratio for this type of CHP unit according to Nilsson [24]. The CHP units power output is defined as

$$P_{CHP} = \alpha Q_{CHP} \tag{1}$$

where α is the power-to-heat output ratio and Q_{CHP} [W] is the heat output. An important aspect when considering CHP generation for power balancing production is the possible rate at which the power output can be varied. This is generally referred to as the ramp-rate, and is defined as the maximum possible degree of output variation in 1 min out of the nominal power output of the unit. This can be expressed as the time derivative of the power output divided by the nominal power. The convention is to express this as percentage of P_n per minute:

$$\varphi = \frac{dP/_{dt}}{P_n} \mathrm{T} \times 100, \tag{2}$$

where P is the power output [W], t is time [s], P_n is the rated nominal power of the unit, and T is seconds per minute, i.e., 60 [s/min]. The ramp-rate depends on the type of burner and the fuel used. For the ORC unit considered in this study a ramp-rate of 4% of P_n per minute is assumed, which is based on a study presented in Wang et al. [25]. Further, to minimize costly starts and stops of CHP units, these often

Table 1
The table shows the relations between installed peak power, share of available roof areas used and the penetration level of installed BAPV. The penetration level assumes that one household installs a "standard-sized" solar panel of 5 kW$_p$.

Steps of increment in simulation		1	2	3	4	5	6	7	8	9	10	11
Penetration level	%	0	2.7	5.4	8.1	10.8	13.5	16.2	18.9	21.6	24.3	27
Share of roof area	%	0	2.5	5	7.5	10	12.5	15	17.5	20	22.5	25
Peak power	kW$_p$	0	15	30	45	60	75	90	105	120	135	150

have a minimum load at which they can be operated. Wang et al. [25] states that similar CHP units as the one considered here can be operated down to 15% of the nominal power output,

$$P_{CHP,min} = 0.15P_n \tag{3}$$

and this percentage is also used in this study. During cold start the unit takes longer time to respond. It was assumed that the unit was optimized for quick response in line with what was reported for CHP units in Denmark [26], i.e., from ignition to 90% of baseload 170 min was required. This was defined as a linear increase of production output during the first 3 h after any period with no production until 90% of P_n was reached. It is described as

$$P_{CHP} = fP_n\frac{t}{\tau}, t = 1, 2, \ldots, \tau \tag{4}$$

where f is a value between 0 and 1 representing the fraction of baseload to reach when full operation is achieved (here the baseload is equal to P_n since the CHP unit is the only production unit), τ is the total start up time in h, and t is hours after start up.

2.2.2. Heat pumps

Central heat pumps for P2H production during VRE production surpluses are here considered a part of the power balancing service provided by the residential area for the national power production. The heat pumps in the study are assumed to have a "high enough" capacity. This means that the thermal output capacity of the heat pumps is defined by the power surplus or the possibility to supply or store heat locally. Also, the heat pumps are assumed to be equipped with variable speed-controlled compressors for rapid response to output variations. This enables the heat pumps to vary their power consumption and heat production at an unlimited rate. This would not be possible in traditional heat pumps where the compressor is an on/off-type and the pump consumes a fixed power level. Hence, the heat pumps here are considered fully flexible regarding power consumption with no specific minimum-load limit. The heat source for the heat pumps is assumed to be ground heat that provides a fairly constant coefficient of performance (COP). The COP is assumed to be constantly at 3.0, which is typical for a ground source heat pump. The produced heat from heat pumps is calculated as

$$Q_{HP} = \eta_{COP}P_{el} \tag{5}$$

where η_{COP} is the COP and P_{el} is electricity, i.e., surplus electricity production from VRE.

2.2.3. Thermal energy storage

The TES modelled for the residential area is a buried cylindrical tank storage with its top in level with the ground surface. A mathematical model of a heat accumulator storage developed by the Swedish Built Environment Research Council [27] was used in the simulations and is outlined below.

The storage and the model parameters are illustrated in Fig. 3. A_i [m^2] is the area of the insulated top of the TES, defined as:

$$A_i = \pi R^2, \tag{6}$$

where R is the radius. A_{ig} [m^2] is the insulated surface underground (walls and bottom), defined as:

$$A_{ig} = \pi R^2 + 2\pi RH, \tag{7}$$

where H is the height of the TES. T_m [K] is the mean temperature at storage surface, T_A [K] is ambient temperature above ground for Uppsala and the year 2014 on hourly resolution [28], and T_u [K] is mean temperature in undisturbed soil. λ [W/mK] is the heat conductivity in the surrounding ground, λ_2 [W/mK] is the heat conductivity of the ground beneath the storage, λ_i [W/mK] is the heat conductivity of the insulation, and d_i [m] is the thickness of the insulation. u_m is a dimensionless factor representing the insulating thickness of the surrounding ground.

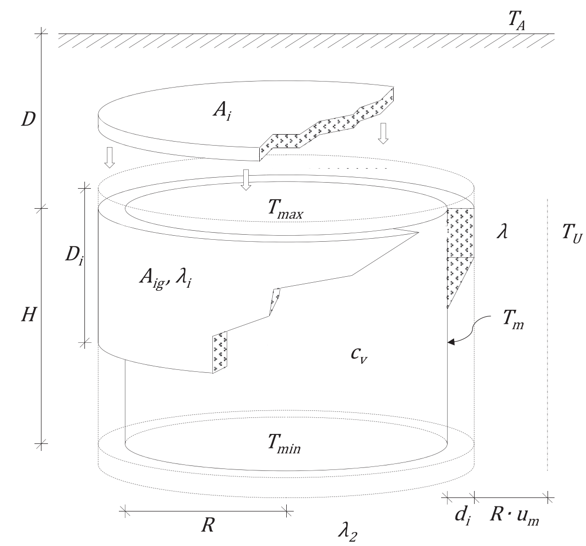

Fig. 3. Schematic description of the thermal storage model. Units are explained in Table 2.

Within the model, stationary conditions, i.e., thermal equilibrium with the surroundings, were assumed. The calculation of the heat losses, Q_m, used the storage surface mean temperature, T_m, over one cycle as representative of the storage surface temperature:

$$T_m = \frac{T_{max} - T_{min}}{2}. \tag{8}$$

This means that the momentary heat losses are based on a mean value representing a longer time period. Thus, the losses may differ on shorter time interval from a real case, but gives a good enough approximation for the full cycle. The losses are described as

$$Q_{m,loss}(i) = A_i\frac{(T_m - T_A(i))\,\lambda_i}{d_i} + A_{ig}\frac{T_m - T_u}{\mathrm{d}_i/\lambda_i + \mathrm{Ru}_m/\lambda}, \tag{9}$$

where the first term is the vertical heat losses through the top of the storage, and the second term is the losses to the surrounding ground. Note that the equation is only valid for $d_i \gtrsim 2d_{min}$, with d_{min} defined as

$$d_{min} = \left(d'_{min}\lambda_i R\right)/\lambda, \tag{10}$$

where d_{min}' is a dimensionless factor based on the storage shape. The reader is referred to Claesson et al. [27] for details.

The dimensions of the storage (height H and radius R) are generated in the simulations. This means that the areas (A_i and A_{ig}) will vary in the results due to the optimal storage size and capacity derived for each of the studied cases (presented in Section 5). However, to maintain a minimal ratio of surface area to volume, which reduces the losses, the ratio of height to radius was kept constant at 2, as this maximizes the volume relative to the surface area for a cylinder. This fixed ratio kept both the parameters u_m and d_{min}' constant (see Table 2).

The energy content in the TES is given by

$$Q_{max} = c_V\Delta TV \tag{11}$$

where c_V is the volumetric heat capacity of water in J/m^{3}K, ΔT is the temperature span between hot and cold temperature in the TES in K, and V is the volume in m^3. The initial volume was set based on the amount of energy required to meet 50% of the thermal peak power demand. During the simulation this was iteratively adjusted to reach an optimal size of the TES (see Section 5).

Table 2
Description of fixed parameters and parameter values used for calculations of storage losses.

Parameter	Unit	Description	Value
D	m	Thickness of the ground above the storage	0
d_i	m	Thickness of the insulation	0.4
λ	W/mK	Heat conductivity of the surrounding ground	1.2
λ_2	W/mK	Heat conductivity of the ground beneath the storage	3.6
λ_i	W/mK	Heat conductivity of storage insulation	0.04
$d_{min}{}'$	–	Shape dependent factor for minimum insulation thickness	0.344
u_m	–	Shape dependent factor for insulating ground thickness	0.7239
T_A	°C	Ambient temperature per hour for 2016 for Uppsala. $\overline{T_A}$:	8
T_m	°C	Mean temperature in the storage	65
T_U	°C	Ground temperature	5
c_v	kJ/ m^3K	Volumetric heat capacity at 90 °C	4059.418

Loading and unloading of the TES have been assumed to have a "high enough" capacity. The energy content over the year in the TES was calculated as

$$Q_{TES}(i) = Q_{TES}(i-1) + Q^{+}_{TES}(i) - Q^{-}_{TES}(i) - Q_{m,loss}(i) \tag{12}$$

for every hour i of the year, where

$$Q^{+}_{TES}(i) = Q_{CHP}(i) + Q_{HP}(i) - Q_L(i) \text{ iff } Q_L(i) < Q_{CHP}(i) + Q_{HP}(i) \tag{13}$$

and

$$Q^{-}_{TES}(i) = Q_L(i) - (Q_{CHP}(i) + Q_{HP}(i)) \text{ iff } Q_L(i) > Q_{CHP}(i) + Q_{HP}(i) \tag{14}$$

This means that in every time step heat loss from storage will be subtracted and/or heat will be stored or extracted depending on the size of the heat demand and the current CHP and/or heat pump production.

The TES performance is measured by the energy efficiency, η_E, that is the share of the energy stored that is later also used and not lost through transmission to the surroundings. The efficiency is defined as

$$\eta_E = 100 \times \left(\frac{\sum_i Q^{-}_{TES}}{\sum_i Q^{+}_{TES}}\right), \tag{15}$$

where $\sum_i Q^{-}_{TES}$ is the annual heat outtake from the storage, and $\sum_i Q^{+}_{TES}$ is the annual amount of heat stored. For a storage that is cycled between maximum depth of discharge and full storage, the degree of utilization, η_U, becomes relevant as it indicates how extensively the storage has been used. It is defined as

$$\eta_U = 100 \times \left(\frac{\sum_i Q^{-}_{TES}}{Q_{max}}\right) \tag{16}$$

where Q_{max} is the nominal capacity of the storage.

2.3. Power balancing demand

This section presents how an approximation is made of a national demand for a power balancing service, and how this is scaled to be represented on the local scale. This power balancing service is basically the VRE deficits and surpluses that the local CHP unit and heat pumps are operated to reduce. The capacity to provide such a service from the local system is, however, limited by the power demand of the residential area, generation from BAPV, and the heat demand in the local DHS. The local power demand and the local BAPV generation are included directly in the definition of the power balancing service demand, while the local heat demand will be indirectly limiting since it limits the potential annual production of heat in the CHP unit and the heat pumps. Furthermore, the balancing service demand (P_{bal}) considers the Swedish power generation mix, and the Swedish power demand. Import and export of electricity are excluded from this definition for simplicity reasons. P_{bal} is defined as

$$P_{bal}(i) = P_{L,local}(i) + C \times P_{bal,nat}(i) - \sigma \times P_{BAPV}(i) \tag{17}$$

where $P_{L,local}$ is the local electricity demand, P_{BAPV} is the local BAPV electricity generation, and σ is a scaling factor representing the share of available rooftop areas utilized for BAPV generation. $P_{bal,\ nat}$ is the national demand for power balancing services, and C is a factor that scales the $P_{bal,\ nat}$ to a representative level for the local system. C is defined as the ratio between the annual local power demand and the annual national power demand. $P_{bal,\ nat}$ illustrates net surpluses and deficits of electricity in the Swedish power production system caused by increased VRE generation and phased out nuclear power, but without dispatchable power production such as hydro or thermal power production. $P_{bal,\ nat}$ is defined as the national electricity demand subtracted with the electricity production from nuclear, wind and solar power as

$$P_{bal,nat}(i) = P_{L,nat}(i) - \left(\varepsilon\left(P_{VRE,add}(i) - P_{VRE,ex}(i)\right) + P_{VRE,ex}(i) + (1-\varepsilon)P_{nuc}(i)\right) \tag{18}$$

$P_{L,\ nat}$ is the national electricity demand. $P_{VRE,\ ex}$ is the existing power generation from wind and PV in Sweden in 2016 [29]. $P_{VRE,\ add}$ is the additional wind and PV added in the scenario cases. The factor ε is used to increase the added amount of VRE in the system ($P_{VRE,\ add}$) and simultaneously reduce the amount of nuclear power (P_{nuc}) in the system. Thus, $\varepsilon = 0$ represents the Swedish 2016 electricity production mix with 11% wind, <1% PV, and 45% nuclear power. Furthermore, $\varepsilon = 1$ represents a mix with 60% wind, 10% PV, and 0% nuclear power (see Table 3).

Fig. 4 shows the electricity production from VRE and nuclear power, national load, and the national electricity balancing service demand for two days in August. The diagrams to the left (A) show a case where $\varepsilon = 0$ (i.e., current electricity production) and the diagrams to the right (B) show a case where $\varepsilon = 1$ (i.e., maximum share of VRE and no nuclear power). Diagrams A_1 and B_1 show the total electricity production from VRE and nuclear power together with the national electricity load, $P_{L,nat}$, while A_2 and B_2 show the resulting balancing demand, $P_{bal,nat}$ as consumption, $P_{L,nat}$, minus production, $P_{nuc+VRE}$ for the two cases.

In diagrams A_3 and B_3 the electricity balance demand profile P_{bal} is shown. $P_{bal,nat}$ is scaled to be represented on local level and added to the locally produced BAPV electricity, $P_{BAPV+VRE}$. From the local power demand, $P_{L,local}$, the produced electricity is subtracted, accordingly to Eq. (17), to give P_{bal}. In diagram A_3 there is no BAPV ($\sigma = 0$) and the 2016 VRE production ($\varepsilon = 0$); thus, P_{bal} is containing the positive residual load (PRL) from both the local demand and the downscaled portion of the national PRL. In B_3 there is no BAPV, but a maximum share of VRE ($\varepsilon = 1$). When subtracting the production from the load one gets the residual load, P_{bal}. Diagrams A_4 and B_4 show the situations as in A_3 and B_3, but with a maximum share of BAPV ($\sigma = 1$). This balancing demand consists of remaining PRL that has not been supplied from the electricity production, but it also consists of excessive electricity

Table 3
The table gives three examples of how ε linearly changes the mix in the power production. VRE generation consist of national PV, PV_{nat} and wind power, Wind. The nuclear power production, P_{nuc} is gradually phased out while the consumption is kept constant. Annual electricity production/consumption are shown as TWh and the electricity peak production/consumption are shown in GW. Please note that the individual peak powers do not coincide in time!

Steps of increment in simulation, ε		0		0.5		1	
		[TWh]	[GW]	[TWh]	[GW]	[TWh]	[GW]
P_{VRE}	PV_{nat}	0.05	0.05	6.1	6.1	13.4	13.5
	Wind	15.6	5.4	36.5	12.7	80.3	27.9
P_{nuc}		60.5	9.1	27.5	4.1	0	0
$P_{L,nat}$		133.8	26.9	133.8	26.9	133.8	26.9

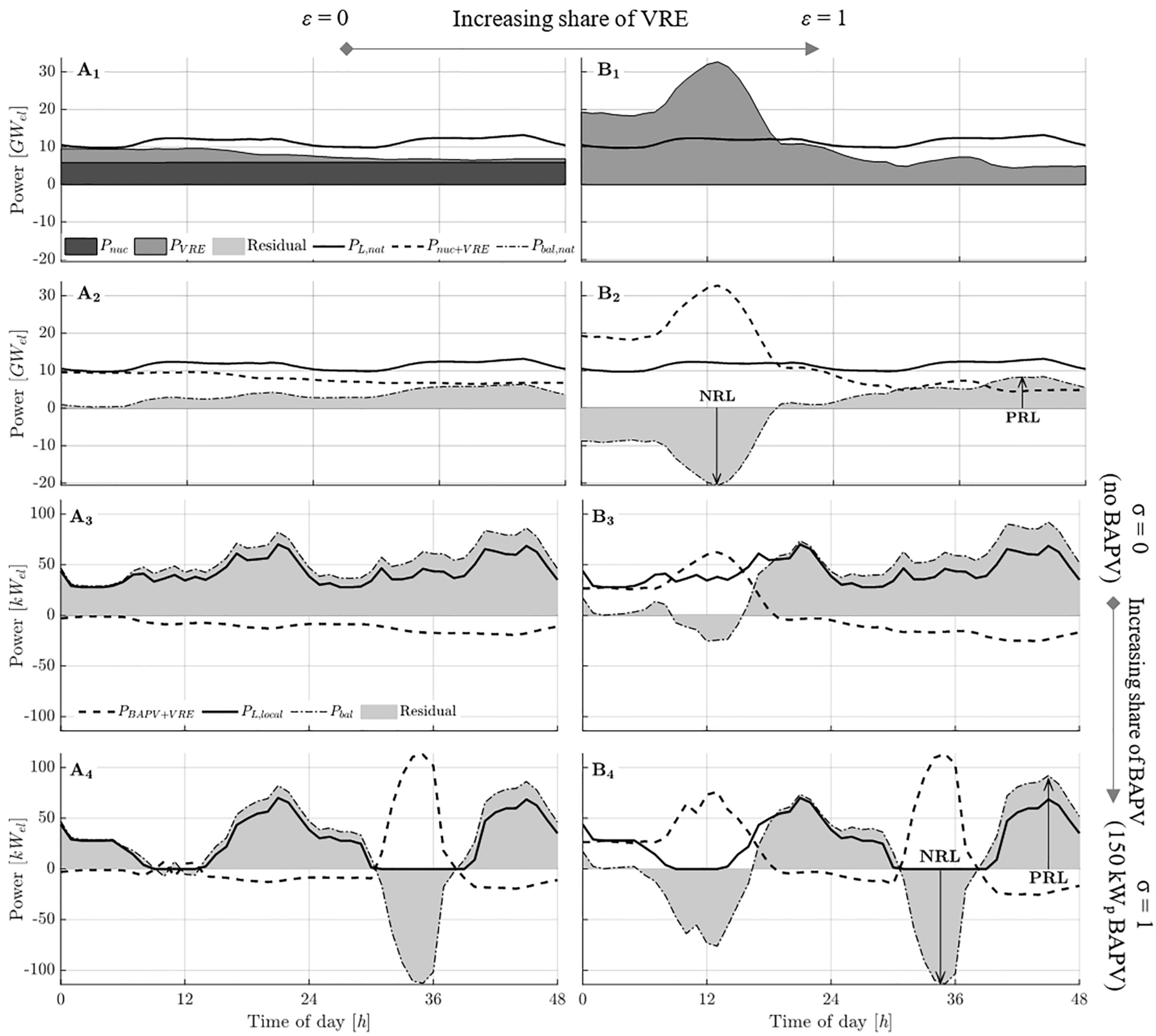

Fig. 4. Construct of power profile shown for two days in August (28th & 29th). $P_{BAPV+VRE}$ in the figure represent the electricity from BAPV (σP_{BAPV}) and $P_{bal,nat}$ ($CP_{bal,nat}$) that represents national power balancing demand due to increased share of VRE.

production giving negative residual load (NRL). In Table 3 is key figures showed for the change in electricity production and peak power capacities.

2.4. Simulation algorithm

It is important to note that the CHP production in the algorithm is primarily operated to meet the power balancing demand. However, most CHP production plants in Sweden are currently primarily operated to supply a district heat demand. This is an important difference between these simulations and conventional CHP plant operation. The power-demand-following CHP production is henceforth referred to as the “Electricity Strategy”. The conventional heat-demand-following production is henceforth referred to as the “Heat Strategy”.

In order to clarify the nomenclature, two parameters will be used extensively throughout the paper: P_{bal}, as defined above, and P_{net}. Both denote electricity net profiles, i.e., consumption subtracted by production, and should ideally be equal to zero. P_{bal} is an intermediate net profile, the result of consumption subtracted with only VRE production and non-balancing power (i.e., nuclear power); hence the index $_{bal}$ for balance, since it represents the electricity balancing profile that requires balancing power utilities to act (e.g., hydro or thermal power). P_{bal} is used as input for the simulations in this study. After running the simulation, the electricity profile has been changed by electricity production (in CHP) and consumption (in heat pumps) and thus results in a new net profile, P_{net}. Hence P_{net} is part of the results in this study. Both P_{bal} and P_{net} will contain residuals, i.e., deviations from zero, both positive (remaining load) and negative (surplus production), varying in magnitude.

The simulation algorithm is designed to level out the heat production over the year. This is achieved by using stored surplus heat to reduce peaks in the local heat demand, Q_L. This enables a reduced need of nominal peak power capacity, P_n, in the CHP unit or additional costly peak load units. This is reasonable, since the power balancing demand would otherwise favor a disproportionately large CHP unit in relation to Q_L. However, as a reduced P_n will also affect the power balancing production capacity, there is a tradeoff between reduced plant investments and providing a power balancing service. In the simulations this is handled by starting with an initial seasonal requirement of a 50% reduction of the peak heat production capacity. If the simulation indicates an insufficiently sized system (e.g., too small TES capacity) the peak reduction requirement is iteratively reduced until no heat deficit occurs in the simulation (which could result in 0% peak reduction).

The simulations also need to handle the conflict of interest between keeping the heat balance versus providing power balancing. First, no waste of produced heat is allowed; all heat produced must be utilized. Secondly, electricity generation from the CHP is prioritized through the 'Electricity Strategy', which inevitably co-produces heat. Third, operators of cogeneration plants want to minimize the number of starts and stops in the plant due to high costs and thermal wear and tear to the plant. Conflicts of interest thus arise in case of very large quantities of surplus electricity that can be used for heat production. If this amount of heat is to be utilized, other heat production must be reduced. If heat pump production becomes particularly extensive, a target conflict arises between maximizing electricity production from the CHP plant (with associated co-produced heat), as well as minimizing the number of costly starts and stops on the one hand, and the reduction of surplus electricity through the operation of heat pumps on the other. In order to reconcile this conflict of interest, the algorithm has a condition that, in the event of excessive heat production, extends the possibility of utilizing all heat produced. This is done by gradually increasing the revision period for the CHP plant during which the plant already is shut down. The effect of this will be less heat production from the CHP plant without costly extra starts and stops, but also that the TES will be used more intensively by increased turnover of the heat in the TES.

The electricity balancing profile, P_{bal}, is used as input data for the simulations together with Q_L. P_{bal} profiles are defined for 11 levels (0–150 kW$_p$) of BAPV, and 12 different levels of nationally generated VRE (corresponding to 11–70% of the annual national electricity production mix). In total, 132 different P_{bal} profiles and simulations for combinations of BAPV and national VRE levels were made.

The decision strategy, i.e. the simulation algorithm, is shown in Fig. 5 and Table 4. The balance profile, P_{bal}, determines whether heat is to be produced in heat pumps ($P_{bal} < 0$), supplied by the TES ($P_{bal} = 0$) or produced in the CHP plant ($P_{bal} > 0$).

$P_{bal} < 0$ means that there is a NRL, i.e. surplus of electricity, to be met by electricity being used for heat production in the heat pumps. The produced heat is primarily used to supply Q_L (i.e., supplied to the DHS), and secondarily stored in the TES. Thus, Q_L and/or the available capacity of the TES might limit the possibility for the system to meet the negative power balancing demand, since the algorithm does not allow heat to be produced and wasted. If the produced heat together with the TES does not cover the Q_L, a heat deficit occurs, indicating that the system configuration is insufficiently dimensioned.

Table 4
Criteria used to optimize the size of the TES. DoD refers to the storage depth of discharge.

Criterion	Option	Action
1. Could all produced heat be stored?	No	Size of TES increased
	Yes	Next criterion
2. Was the amount of heat available in TES sufficient to supply the seasonal peak shave, i.e. replace peak load production?	No	Reduce the peak shave
	Yes	Next criterion
3. Is the energy content in the TES at the end of the year less than in the beginning of the year (heat drainage)?	Yes	Reduce the peak shave
	No	Next criterion
4. Is the energy content in the TES at the end of the year >110% of the energy content in the beginning of the year (heat accumulates)?	Yes	Extend the revision of the CHP (increase usage of TES)
	No	$Q_{TES,max}$ defined. Next criteria
5. Does the DoD reach $0 < Q_{TES} < 0.1Q_{TES,max}$?	No	Reduce initial energy in TES
	Yes	Next criterion
6. Does the fully loaded TES reach $0.9Q_{TES,max} < Q_{TES} < Q_{TES,max}$?	No	Reduce TES size
	Yes	TES optimally dimensioned

When $P_{bal} = 0$, the production and consumption are balanced, thus there is no power balancing demand. Q_L is in this case covered by heat from the TES. Here is also a possibility that Q_L cannot be covered by heat from the TES, i.e., a heat deficit might occur. This would also lead to an indication that the system configuration is insufficiently dimensioned.

Finally, if $P_{bal} > 0$, there is a PRL that calls for power production in the CHP unit. The co-produced heat from that power production is, as for the heat pump in the first case, primarily used to cover the Q_L and secondarily, if TES capacity exists, stored. If no capacity is available in the TES the power production in the CHP unit will be limited by this and the power balancing demand is not completely met. The CHP unit is also restricted to co-generation of power and heat. Thus, it cannot be operated for heat-only or power-only production. If the co-produced heat and available heat from the TES is less than Q_L a heat deficit occurs, again indicating that the system configuration is insufficiently dimensioned.

The decision strategy described in Fig. 5 is performed on hourly

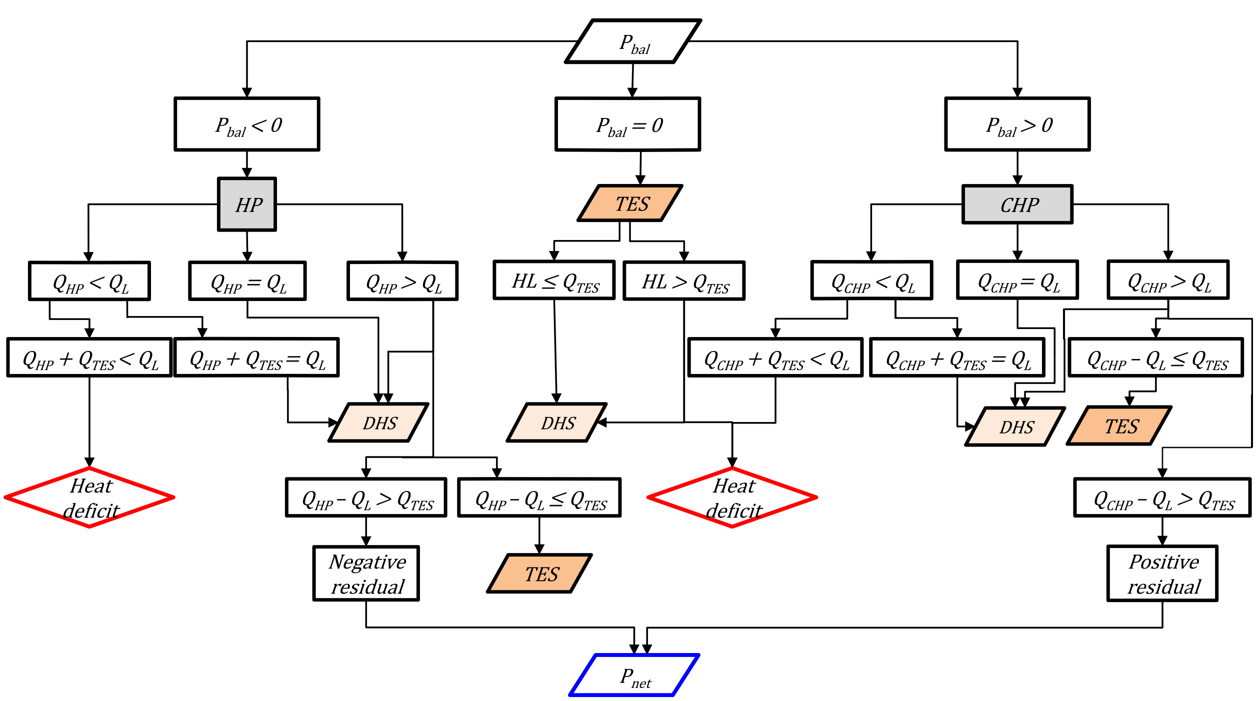

Fig. 5. Schematic decision process in the model. *HP* is abbreviation for heat pumps and Q_L is the local heat load.

resolution for a full year. In the algorithm Q_L is used to calculate an estimated initial size of the TES. This is done by assuming that the seasonal 50% shaving of the peak Q_L is to be performed with the help of the TES. The initial energy content in the TES is set to be 85%. At the end of the simulated year the performance of the TES is analyzed by a set of criterions to determine if it has been optimally sized (see Table 4). The criteria come in sequence were subsequent criteria are dependent on the fulfilment of the previous one. The fulfilment of the criteria is done iteratively (i.e., when a correction has been made to reach a criterion the algorithm is run for a full year again until the criterion is fulfilled), and criterion by criterion. After each iteration all the previous criteria must be checked before advancing to the next one.

3. Results

The presentation of the results is divided into three sections; *power balancing supply*, *local system heat balance*, and *TES sizing and performance*. Also, extra attention is paid to the simulated case with maximum amounts of national VRE and BAPV generation, i.e., the 132nd (last) simulation. This case is interesting due to its large amounts of VRE generation and is henceforth referred to as "Case 132".

3.1. Power balancing supply

The results for how the power balancing demand is supplied in the simulations are presented in this section, initially in detail for Case 132 and then more generally for all simulated cases. In Fig. 6, it is shown how the power balancing services are provided by the local energy system for Case 132. Fig. 6A shows a duration graph for the ingoing power balancing demand, P_{bal}, and the resulting net profile, P_{net}, after the local energy system's provision of power balancing services. In Fig. 6A it can be seen that during 2800 h the local energy system setup manages to fully balance the electricity balancing demand, i.e., $P_{net} = 0$. Out of these, almost 1100 h of balancing were achieved through production in the CHP unit. It is also shown that during 1700 h the negative residual was fully consumed by heat pumps for heat production.

Fig. 6B shows the correlation between the power balancing services (CHP and heat pumps), and P_{bal}. A perfect match between production and demand is indicated by the diagonal grey line. It can be seen that the CHP unit produces electricity at its peak capacity of 32.4 kW$_{el}$ during significant part of the time (4676 h, not visible in the graph). The 2800 h of perfect balance are indicated in the figure by data points on the diagonal matching line for production and consumption in the CHP and heat pumps respectively. The three scattered datapoints for CHP production correspond to the cold start of the CHP unit after revision (it took 3 h until 90% of P_n was reached).

In Table 5 key figures for Case 132 are shown. The peak CHP electricity output, P_n, for the 'Electricity Strategy' is 32.4 kW$_{el}$. This is a result of the iterative dimensioning of the CHP unit and the TES described in Section 5. All of the negative residual load and 43% of the positive residual load were reduced. The peak power deficit was reduced by 21% and the peak surplus was reduced by 100% as shown in Table 5. The reduction of the peak NRL benefited from the unrestrained size of heat pumps. The peak PRL in P_{bal} occurred in the end of January and was reduced with the CHP unit's P_n (32.4 kW$_{el}$) to 119.6 kW$_{el}$. The capacity factor was 0.64 for the CHP unit.

Fig. 7 shows the dynamics of the power balancing demand, the CHP production, and the electricity use in heat pumps for Case 132, during one week in April. It is clear that the maximum capacity of the CHP unit limits its possibility to provide a power balancing service. The electricity used in the heat pumps to reduce VRE surpluses meets all of the negative power balancing demand (light grey areas). The white area between the grey areas and the P_{bal} curve is the remaining power balancing demand, also shown as the black P_{net} curve. Fig. 7 shows how the CHP unit only produces electricity when there is a positive residual. It also shows that whenever the BAPV systems produce electricity exceeding the load, the heat pumps are used as flexible load to consume surplus power.

Fig. 8 shows the annual amounts of ingoing positive/negative residual loads in P_{bal} before the simulation (PRL$_{before}$ & NRL$_{before}$) and the resulting remaining positive/negative residual loads in P_{net} after the simulation (PRL$_{after}$ & NRL$_{after}$). Fig. 8A and B show the cases with minimum and maximum shares of VRE, respectively, under varied amounts of installed BAPV. Fig. 8C and D show cases with no BAPV and maximal installations of BAPV, respectively, for varying shares of VRE.

In Fig. 8 it can be seen that in all cases the simulation reduced the

Table 5
Key figures for Case 132. Positive residual load, PRL, is the remaining power demand after subtracting the electricity production from the consumption. Negative residual load, NRL, is the excess electricity production that when subtracting the electricity production from the consumption becomes a negative residual.

	PRL		NRL	
	[kW$_{el}$]	[MWh$_{el}$]	[kW$_{el}$]	[MWh$_{el}$]
P_{bal} (before simulation)	152	405	181	104
P_{net} (Case 132)	120	233	0	0
Diff [%]	−21	−43	−100	−100

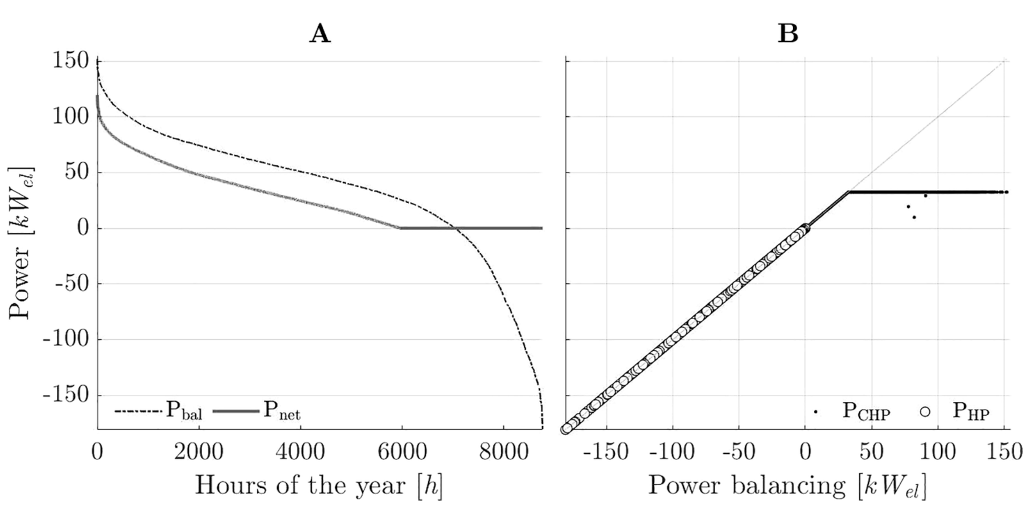

Fig. 6. Figure A shows duration graphs for ingoing P_{bal} and resulting P_{net} for the proposed 'Electricity Strategy' in Case 132. In figure B is the matching of power balancing shown. The straight diagonal line in B indicates a perfect match between production and demand.

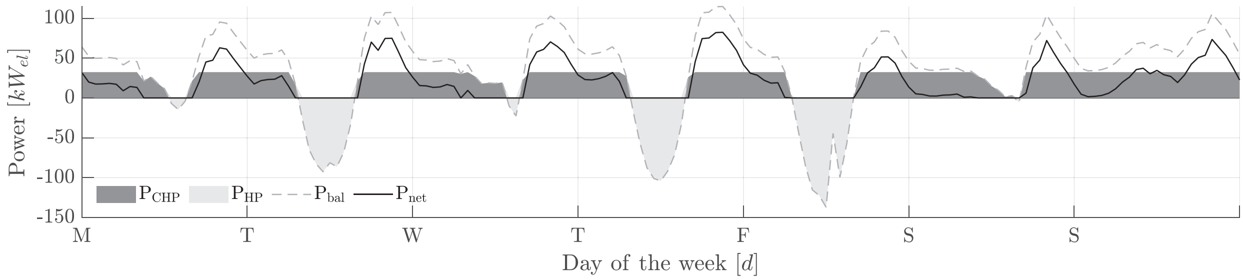

Fig. 7. Electricity production in CHP, P_{CHP}, and consumption in heat pumps, P_{HP}, for Case 132, during one week in April.

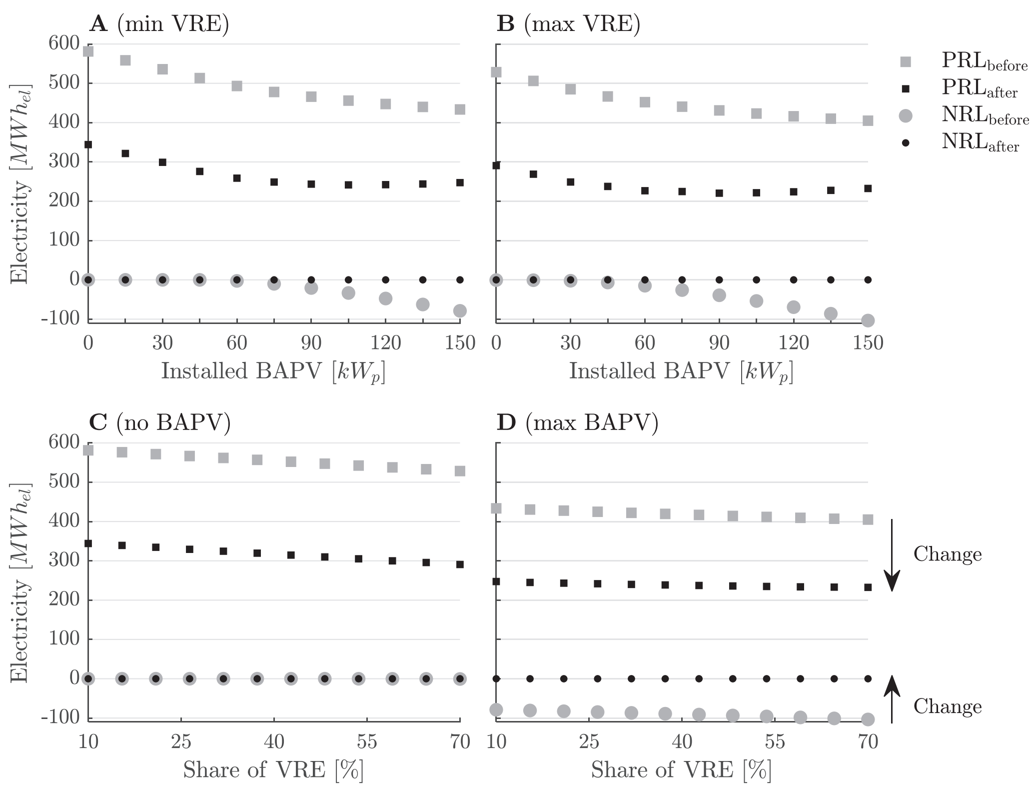

Fig. 8. Annual electricity positive and negative residual loads before (P_{bal}) and after (P_{net}) the simulation.

amounts of both positive and negative residual loads when compared with ingoing deficits/surpluses. It is also clear that the electricity demand is significantly higher than the surplus electricity.

After applying the proposed 'Electricity Strategy' the CHP power generation reduces the positive power balancing demand on average by 46% (min 41%, max 50%) for all 132 simulated cases. Negative power balancing demand has been reduced by consumption in the heat pumps. As shown in Fig. 8D, with maximum level of BAPV installations, the NRL_{after} is completely reduced for all cases of different shares of VRE. This means that the system is capable of handling the approximated surplus of VRE production from both BAPV and other VRE production on national level.

Furthermore, 8A and 8B, show that with an increase of installed BAPV follows a decrease of ingoing electricity demand, but at levels of 60 kW_p BAPV installations this effect levels out. This is clearly visible for the remaining positive residual load after the simulation (PRL_{after}). This is explained by the fact that with increased amount of installed BAPV comes an increased time-related mismatch between demand and supply. This causes an increasing amount of surplus power for the heat pumps to consume. In the figure this can be seen as an increasing amount of ingoing negative residual load (NRL_{before}) at the same level of installed BAPV (60 kW_p).

It should be clarified that with a minimum share of VRE in the national power production the total power production from nuclear and VRE together only correspond to approximately 50% of the national power demand. In the simulations nuclear power has been phased out and replaced with increased production from VRE. With a maximum share of VRE, nuclear power no longer contributes with any power production, but the annual VRE now instead corresponds to 70% of the national demand. This means that the annual power production has increased significantly, but due to the volatile nature of the power sources there has not been an equally large decrease in the ingoing power demand (PRL_{before}). In 8C the change between minimum and maximum share of VRE is shown, corresponding to a reduced electricity demand of about 9% (52.7 MWh_{el}). However, the possibility for the local CHP unit to perform power balancing production is not affected by this.

Fig. 9 shows the peak ingoing positive and negative residual loads in P_{bal} before the simulation (PRL_{before} & NRL_{before}) and the resulting remaining positive and negative residual loads in P_{net} after the simulation (PRL_{after} & NRL_{after}). Fig. 9A and B shows the peak powers for cases with minimum and maximum share of VRE respectively during varied amounts of installed BAPV. Fig. 9C and D similarly show the peak powers for cases with none and maximal installations of BAPV, respectively, under varied shares of VRE.

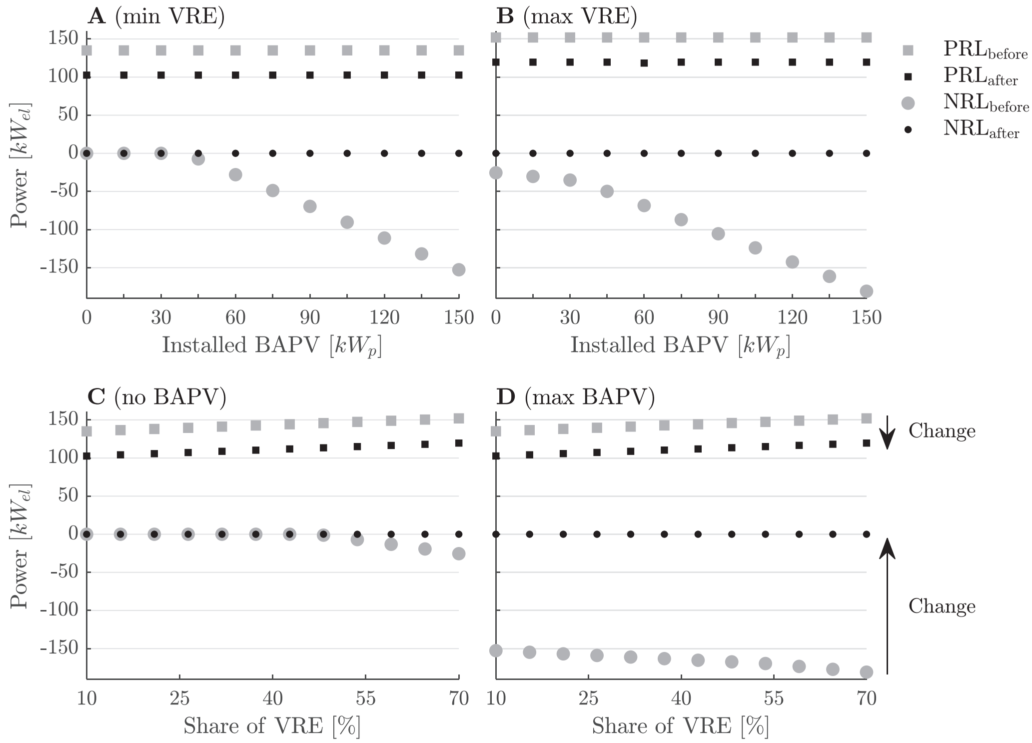

Fig. 9. Positive and negative residual peak loads before (P_{bal}) and after (P_{net}) the simulation.

In Fig. 9 it can be seen that in all cases the simulation reduced the peak powers for both positive and negative residual loads when comparing with ingoing deficits and surpluses. It is also clear that the ingoing deficit peaks in P_{bal} (PRL_{before}) are fairly constant in all different cases whereas the ingoing surplus peaks in P_{bal} (NRL_{before}) vary significantly.

The remaining peak demands for the positive residual load in P_{net} correspond to an average peak reduction of 22.6% (min 21%, max 24%) of the ingoing peak demands in P_{bal}. In 130 cases the peak demand is reduced with 32.4 kW_{el}. This equals the reduced P_n for the CHP unit which was achieved since the TES covers the peak demands. The remaining two cases had a slightly higher reduced peak demand of 33.6 kW_{el}. The reason for this is that excess heat from co-production and/or P2H in these two cases were not sufficient to enable the TES as thermal peak load capacity corresponding to 50% of the thermal peak demand during the peak load season. It could only cover 48% of the thermal peak demand, hence the CHP unit's P_n became slightly higher (33.6 kW_{el}) in these two cases. A way to compare a power producing units' performance is the capacity factor. For a CHP unit operating in a DHS the traditional operating strategy is to follow the heat demand, i.e., the co-generated electricity is a by-product to the produced heat. This is reflected in the capacity or load factor of a cogeneration unit, which in these cases can be as low as 0.25, while a cogeneration device intended only for power generation can reach capacity factors >0.8. In this study the capacity factor for the CHP unit on average became 0.81 (max 0.89, min 0.64).

Fig. 9A and B shows that the peak power of the positive residual loads in P_{bal} (PRL_{before}) does not change with increasing amount of BAPV (in contradiction to the corresponding annual amounts presented in Fig. 8A and B). This confirms the somewhat intuitive result that the peaks of the power demands do not generally coincide with BAPV production. This is because power demand in residential buildings normally is higher during early mornings, evenings and generally during the darker period of the year, which is an also unfavorable time for PV production.

On the other hand, the magnitude of the peak power for negative residual loads in P_{bal} (NRL_{before}) depends heavily on the level of installed BAPV. This is explained by the temporal mismatch between demand and supply causing surpluses of BAPV electricity. The share of national VRE production has less impact on the NRL peak power. With already 60 kW_p BAPV installed these causes a negative peak power of 28 kW_{el} when the share of VRE is at its minimum (see Fig. 9A). All peak powers of the negative residual loads in P_{bal} had been reduced after the simulation by electricity consumption in heat pumps. Maximum electric power use in heat pumps is 181 kW_{el} in Case 132.

3.2. Local system heat balance

The heat production in CHP and heat pumps for the simulated cases is presented in this section, in detail for Case 132 and more generally for the other cases. The annual heat production in the CHP for the 'Heat Strategy' is 1140 MWh_{th} with a required peak load capacity of 323 kW_{th} in all cases. In general, the 'Electricity Strategy' results in a reduced required peak capacity for the CHP unit in all cases. This is a result of the chosen strategy where the TES is used as a seasonal storage to cover the cold season's thermal peak demands, i.e. seasonal peak shaving. This strategy could replace costly alternative peak production capacities. It also enables a more appropriate dimensioning of the production unit all year around. For 130 cases the capacity is reduced by 50% of the nominal power, P_n, i.e., from 323 to 162 kW_{th}. For the remaining 2 cases, the peak power is reduced by 48%. These 2 cases both have 60 kW_p BAPV installed and maximum share of VRE.

Table 6 shows the results for the heat balance in Case 132 under the 'Electricity Strategy' compared to the 'Heat Strategy'. The total heat

Table 6
Key figures for the heat production in Case 132.

	[MWh_{th}]	Q_L	Q_{CHP}	Q_{HP}	Q_{TES}
'Heat Strategy'		1140	1140	–	–
'Electricity Strategy'	To DHS	1140	764	105	271
	To TES		121	206	327
	Total production		885	311	–

production in the CHP unit is 22% less (885 MWh_{th}) with the 'Electricity Strategy'. About 121 MWh_{th}, or 13.7%, of the heat produced in the CHP was stored, which is 37% of the total amount of stored heat. The other 63% were produced in heat pumps.

Fig. 10 shows the duration for heat production and supply of heat to DHS for Case 132. In A, the total heat produced in the CHP unit, Q_{CHP}, and in the heat pumps, Q_{HP}, are shown together with the heat load, Q_L. It is clear that access to TES enabled a reduction of the required peak capacity in the CHP by 50% to 162 kW_{th} instead of 323.4 kW_{th}. It can be seen that the CHP unit produces at its max capacity during 4600 h and partly during periods when Q_{CHP} exceeds Q_L. The heat pumps produced heat for some 1700 h during the year with a peak production of 543 kW_{th}.

Fig. 10B shows heat supplied directly to the local heat demand (from CHP, heat pump, or TES). The CHP unit covered 67% of the local heat demand by direct supply. The remaining heat demand was covered by the TES (24%) and the heat pumps (9%). Fig. 10B also indicates that the CHP production was low when the heat demand was low, typically during summer, and that the heat pumps and the TES were used for peak- and low-load hours. The low-load hours are normally in the warm parts of the year, which also coincides with peak generation from BAPV and thus also a surplus of VRE for the heat pumps to consume. The low heat load and the large VRE surplus mean that the share of heat pump heat to be directly supplied for the local heat demand is limited. The TES thus is important for the possibility of providing power balancing service by consuming surplus electricity.

In both 10A and B it can be seen that the CHP unit was operational during 6716 h of the year. During the remaining 2044 h the unit was shut down (about 12 weeks). The heat demand was during this time supplied with heat produced in the heat pumps or from TES. The down time period for the CHP started in the beginning of June and lasted until second half of August.

Fig. 11 shows the heat supplied (Q_{CHP}, Q_{HP}, and Q_{TES}) in Case 132 to cover the local heat demand, for the same week in April as in Fig. 7. The CHP unit co-produces heat for the local heat demand or the TES when $P_{bal} > 0$, i.e., when there is a net electricity demand. The CHP output is limited to 162 kW_{th}. When the local heat demand is higher than the CHP output capacity, heat is supplied from the TES. When $P_{bal} < 0$, i.e., when there is an electricity surplus, heat pumps are used. It is clear from Fig. 11 that when the heat pumps are used, the CHP produces at its minimum load, i.e., no power is generated in the CHP unit since there is a negative power balancing demand.

Fig. 12 shows the share of total annual heat production produced in the CHP and heat pumps, respectively, for all simulated cases. The graph shows the cases in 11 blocks. Each block represents a certain level of BAPV. Furthermore, each block contains 12 bars that represent the different levels of VRE (indicated with the double arrow). The results show that close to no heat is produced in the heat pumps for BAPV installation levels below 45 kW_p. This is because these low levels of BAPV contain very little VRE surpluses for the heat pumps to use, and that the CHP therefore covers the entire heat demand. Heat from heat pumps that supplies the local heat demand increases with increased BAPV. In Case 132 the heat production in the heat pumps represents about 26% of the total heat production.

The total heat production in heat pumps for the cases with a maximum VRE scenario increases nearly linearly with an increased installation of BAPV. This means that the TES contributes with a flexible heat load enabling increased power balancing service for these cases.

3.3. Thermal energy storage sizing and performance

The sizing and performance of the TES depend significantly on the strategy used for loading/unloading heat to and from the TES. Here, the TES was used to promote a seasonal levelling of the heat demand, while also using it on a diurnal time-scale. The focus has, therefore, not been to maximize the cycling of the storage on shorter timescales.

The volumetric size of the TES is strictly related to the energy capacity of the storage. Fig. 13 shows the volumes of the TES for all simulated cases. The size of the TES varied between the different cases, from 2000 m^3 to 3250 m^3 (10.4% to 16.1% of the total heat demand, Q_L, respectively). Note that the size of the storage is slightly smaller for levels below 75 kW_p BAPV installed compared to storage sizes for levels >75 kW_p BAPV, i.e., 2100–2900 m^3 (10.4%–14.6% of Q_L) and 2300–3250 m^3 (11.4%–16.1% of Q_L) respectively. For all levels of installed BAPV the size of TES is strongly related to the share of VRE. At levels >90 kW_p BAPV the share of VRE still is a crucial factor for determining the size, but the access to larger negative residuals from BAPV leads to a larger size even with low shares of VRE. The largest volumes are for the cases with high levels of BAPV and high shares of VRE. This correlates well with large power surpluses causing high quantities of produced heat from heat pumps to be stored (see Fig. 12).

Through all simulations it was unambiguously so that heat losses from the TES increased with an increased storage volume. The heat losses varied between 35.5 and 46 MWh_{th} (on average 40.5 MWh_{th}). The mean of the relative losses, i.e., the share of heat supplied to the TES that is lost, Q_{loss}/Q_{in}, was 16.5%. The variation among the cases for the relative losses was ranging from 13% to 21%. The relative losses were generally higher in cases with low share of VRE and small amounts of BAPV. Basically, all cases with maximum share of VRE, and all cases with >105 kW_p BAPV had relative losses below average (<16.5%).

The energy efficiency, η_E, for the TES varied between 75% and 85% (mean 80%). With smaller amounts of BAPV installations (<45 kW_p), η_E

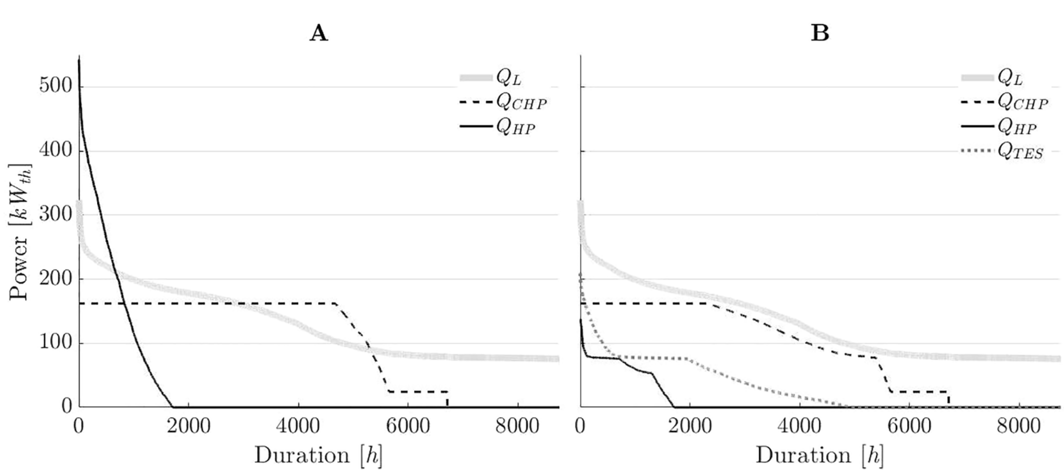

Fig. 10. Duration graphs for Case 132 of heat production in CHP and heat pumps (A), and heat delivered to DHS (B).

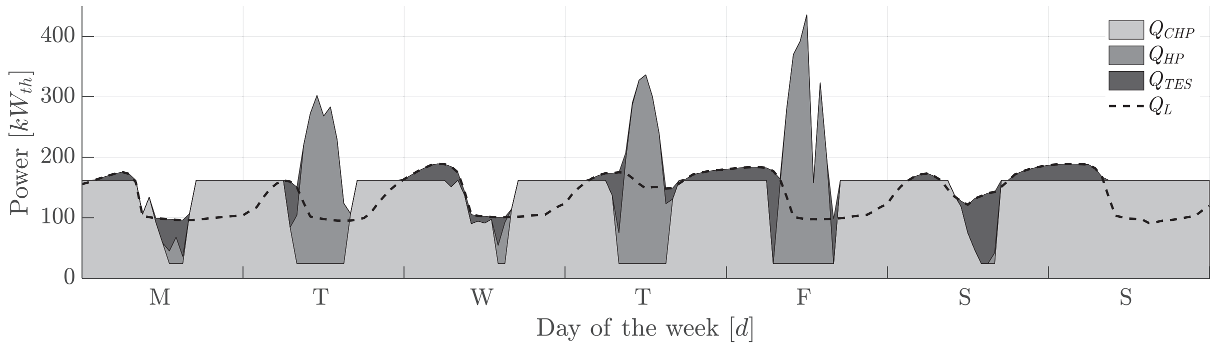

Fig. 11. Distribution of heat sources to DHS during a representative week in April for Case 132.

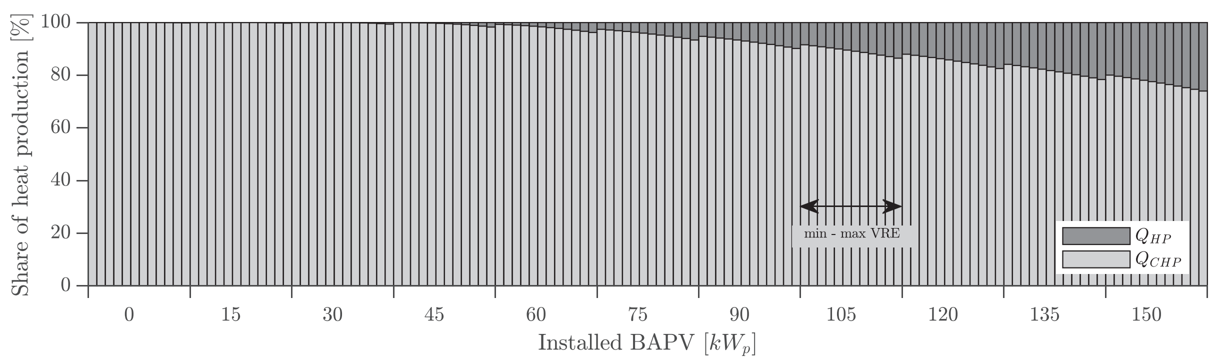

Fig. 12. Distribution of heat produced from CHP and heat pumps as share of all heat produced for all cases simulated.

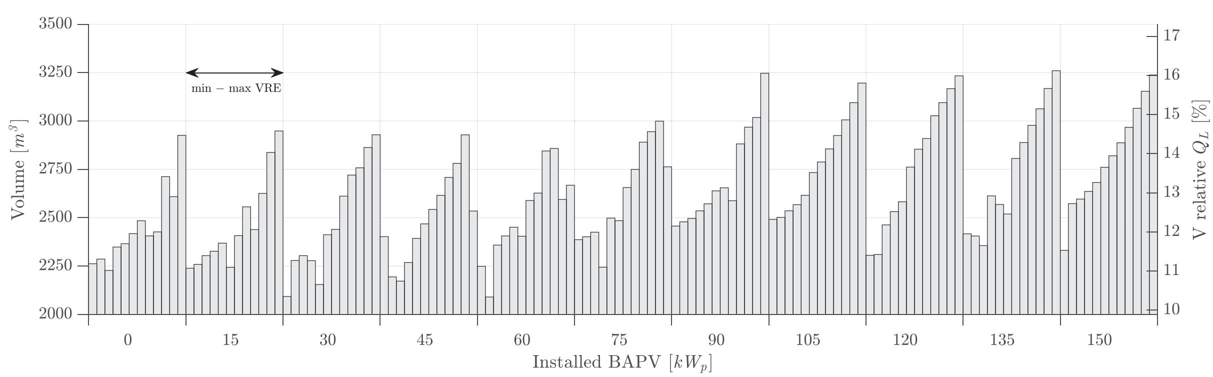

Fig. 13. Volume of storage (N.B. y-axis does not start at zero!). Right y-axis shows energy content relative to total heat load, Q_L.

strongly follows the share of VRE (varying between 75% and 80%). For installations >45 $kW_p \eta_E$ is holding steadier around 81% with a slight trend of increment with larger amounts of BAPV. This is related to the cycling time of the TES, i.e., the degree of utilization, η_U. In average the degree of utilization is 135%, meaning that the storage is cycled slightly >1.3 cycles over the year. The peak of η_U (reaching 182%) occurred for the case with minimum share of VRE and 150 kW_p of installed BAPV. The η_U varied significantly (between 106 and 182%). Generally, η_U increases with the amounts of BAPV, but η_U also generally decreases with higher share of VRE. The η_U is directly dependent on the chosen operational strategy for the TES. The shorter cycling time, the greater η_U. With the strategy in this study of consuming all NRL in heat pumps the extent of time during which the CHP unit was shut down and the TES and/or heat pumps solely supplied heat to the DHS, varied significantly, and thus also the cycling time in the TES.

4. Discussion

In this section, the implications and limitations of the results, the methods and materials, and the assumptions made for the VPP components, are discussed.

The results presented in this paper indicate that power balancing issues due to large shares of VRE in power generation mixes could be decreased and to some extent prevented by incorporating balancing functions on a distributed and local level. The results should be considered applicable primarily for local residential single-family house areas. However, VPPs with CHP, HPs and TES can possibly be implemented also for larger urban residential areas and city districts, especially where DHS are already in place. And, as mentioned in the introduction, DHSs have been built in most Scandinavian cities. Therefore, the potential for using VPPs for power balancing, at least in Scandinavia, should be considered significant.

As mentioned in the introduction a limitation for this study is that it has a technical approach and does not consider economic or policy aspects that might influence the system performance. An operation strategy based on minimizing production costs will not necessarily promote reduction of VRE deficits and surpluses. As shown in Åberg et al. [30], current price mechanisms for electricity on the Nordic electricity market is not an optimal regulation mechanism for matching P2H electricity use for district heating production to VRE production peaks.

There are, however, examples of heat pumps and CHP units that have been operated based on current electricity market pricing. In Stockholm, the local energy company has used reduced power consumption in heat pumps as bids on the regulating market as described in Levihn [31]. Also, CHP units have been participating in regulating power markets in the Nordic power system as described in [32]. Furthermore, there are ongoing projects to modify pricing on electricity markets in order to adequately price capacity reserves within the EU initiated project CoordiNet [33]. This indicates that on future markets for energy, the conditions for implementing the type of system investigated in this study might be better than today. This is also supported by results presented in Helin et al. [34]. Even though that study considers a traditional production strategy for CHP, the authors noted that a capacity driven market is of increasing relevance for the future Nordic energy market with an increased share of VRE.

The results show that the size and variations of the heat demand strongly influence the capacity for a VPP to provide balancing services, but that a TES can increase the potential for reducing the power balancing demand (both negative and positive residual loads). This is in line with results for P2H production presented by Schweiger et al. [11], and with the discussion regarding the limits of heat demand for P2H production potential in Böttger et al. [10]. However, the results presented here show more specifically that a seasonal TES and prioritized P2H production increase the capacity to reduce negative residual load. CHP power balancing capacity, on the other hand, is limited by a seasonal TES, which covers the heat demand peaks and therefore reduces the required heat production capacity of the CHP. A short-term storage strategy could possibly have increased the reduction of the positive residual load, but at the expense of decreased reduction of the negative residual load. This would, however, also require installation of a larger and more expensive CHP unit. These findings reveal further insights in the complexity of combining P2H and CHP with a TES for power balancing, and that the use of the TES (long-term or short-term) is crucial for the system performance.

Another important aspect regarding the heat demand is the conflict between improved energy efficiency in buildings and the capacity for CHP and P2H to provide power balancing services. A higher energy efficiency in buildings reduces the heat demand, and thus further limits the capacity for reducing residual loads. In this study the improvement of energy efficiency in buildings is prioritized, i.e. the energy efficiency of the buildings is assumed to have been significantly improved. A different priority, where energy efficiency measures are avoided, would likely increase the potential residual load reduction. This trade-off, and the risk of locking the system into a higher-than-necessary heat demand need to be considered when designing a system of this type.

The power balancing demand used in the calculations is approximated using power generation data for 2016. This means that the VRE production profile and, thus, the power balancing profile reflect the wind and solar power generation conditions in 2016 and for the sites where wind and PV power production units were installed that year. The power balancing demand will differ between years due to varying weather conditions. However, there is reason to believe that the variability in the power balancing demand will be smaller with a more widespread addition of VRE capacity. This is due to the smoothing effect resulting from having VRE units evenly distributed over a large geographical area (cf., for example, Widén et al. [35]). The power balancing demand approximated in this paper can therefore be expected to slightly underestimate the potential for using a VPP to reduce the power balancing demand.

There are, however, more aspects to consider. The capacity needed for additional power balancing will depend on the water reserves for hydro power production. Hydro is the primary power balancing in the Scandinavian countries. The difference between a hydrologically dry and wet year implies that the balancing capacity of Swedish hydro power can differ about 20% from a hydrological normal year [36]. Furthermore, in recent years, several Swedish (c.f., for example SvK [37] or Länstyrelsen [38]) as well as European cities have experienced power capacity shortage due to limitations in the transmission between national and regional power distribution networks [33]. This means that hydro power in Sweden can necessarily not supply power balancing demands in distant urban areas. Thus, local VPP solutions can play an important role to increase VRE generation within urban areas.

Some simplifications are made in the model that might have implications for the results. For example, the power-to-heat ratio of CHP units varies to some extent depending on the heat output [39], whereas in this study it is assumed to be fixed. However, as the variation has been shown to be within 10% for Swedish CHP units [40], the assumption is thought to be accurate enough for the purpose of this study.

Furthermore, perfect forecasts are assumed in this study. This means that, for the simulations, hourly heat and power loads for the entire year are known. Therefore, the results presented should be considered as a technical potential for the VPP to provide power balancing services. Heat and power loads might vary to some extent between years due to differences in average outdoor temperatures, but the variations between seasons and for shorter time-periods are generally similar between different years. The general performance of the VPP and the patterns in the residual load reductions can, thus, be considered to be generally valid. A further development of the study would be to apply a stochastic forecasting model to forecast the production strategy, based on historical and temporal data. Such an analysis would be valuable to test the robustness of the production strategy.

Even though a DHS is considered in this study, the system configuration presented should also be generally applicable to a similar area with a district cooling system, i.e., for latitudes with a high cooling demand instead of a heating demand. In that case, heat from CHP and heat pumps could be used in a sorption chiller to produce cooling. For higher efficiency, heat pumps could use the return flow from the district cooling system as heat source. The TES would then instead store cooling. The conversion losses would most likely be higher since the sorption chiller adds a conversion step. On the other hand, the thermal losses as well as the distribution losses could be lower due to lower temperature differences. The energy balance and performance of such a system, however, needs further studies, since energy demands, conditions for electricity production, and system component efficiencies might differ significantly from the Nordic conditions.

5. Conclusions

This study showed how a virtual power plant (VPP) in a local residential area with single-family houses can provide power balancing services to a power system with large shares of variable renewable electricity (VRE) generation. The VPP consisted of local building applied photovoltaics (BAPV), a small-scale combined heat and power (CHP) unit, heat pumps, a thermal energy storage (TES), all of which were connected to local district heating and power systems.

The main contribution of this study is that it shows that there is a technical potential for conventional DHS infrastructure to provide local positive and negative power balancing capacity, and that an unconventional operation strategy for DHS utilities is necessary to realize this potential. Literature suggests that this, in turn, would require development of unconventional energy market structures.

The results show that the simulated VPP could provide a power balancing service within the national system. The approximated annual and peak electricity deficits due to large shares of VRE would be reduced by 46% and 23%, respectively. The annual and peak surplus electricity were both fully reduced. Even though the exact numbers are largely influenced by the specific area studied and the system components considered, the results indicate that VRE generation can be increased and that power balancing services can be provided by integration of heat and power systems on a local residential area level.

The TES component of the system is crucial for the possibility to shift the local heat demand in order to reduce the limiting impact that the heat demand has on the possibility to provide power balancing service. The results presented here indicate that the optimal size of the TES depends on the characteristics of the VRE generation in the system. In this study the energy content in the TES corresponded to 10–16% of the annual heat demand. Heat produced in heat pumps using surplus from BAPV generation mainly motivates a seasonal storage. However, a VRE mix with a balance between BAPV generation and a national VRE production with a larger share of wind power could motivate a smaller TES that is used for storing heat on a shorter term.

The heat losses from the TES and the efficiency of the storage under the system operation simulated here were about 16.5% of the heat stored. The efficiency of the storage is about 80%. This is in line with previous studies in the field. Also, the results were quite similar for different sizes of TES and for different user frequencies.

The results also indicate that a system with CHP and a TES reduces the required installed heat output capacity of the CHP unit. This, however, is also on the expense of possible balancing power produced to cover power deficits and highlights the tradeoff from the different possibilities to optimize these types of systems. It can also be argued that the combination of CHP, heat pumps, and a TES also provides a heat production resilience for the system. The need for back-up heat production capacity is significantly reduced with this setup. Furthermore, the results indicate that heat pumps and TES can aid in decarbonization of the energy system by enabling an increased share of VRE. In the cases with the highest share of VRE and BAPV, >20% of the heat production in the CHP unit were replaced with heat from heat pumps, partially through utilization of the TES.

CRediT authorship contribution statement

Svante Monie: Conceptualization, Methodology, Software, Formal analysis, Writing - original draft. **Annica M. Nilsson:** Methodology, Resources, Writing - review & editing. **Joakim Widén:** Resources, Writing - review & editing. **Magnus Åberg:** Conceptualization, Methodology, Resources, Writing - review & editing, Supervision.

Declaration of competing interest

The authors declare that they have no known competing financial interests or personal relationships that could have appeared to influence the work reported in this paper.

Acknowledgements

This study has been carried out partly within the research project “Energy storages for regional and local integration of heat and power systems” (project number P42904-1), financed by the Swedish Energy Agency. This work also forms part of the Swedish strategic research program StandUp for Energy.

References

1 UNFCCC. Adoption of the Paris Agreement. Report no. FCCC/CP/2015/L.9/Rev.1, UNFCCC; 2015. http://unfccc.int/resource/docs/2015/cop21/eng/l09r01.pdf.
2 EUR-Lex - 52019DC0640 - EN - EUR-Lex, n.d. URL https://eur-lex.europa.eu/legal-content/EN/TXT/?uri=CELEX:52019DC0640 (accessed April 7, 2020) [WWW Document].
3 Du P, Baldick R, Tuohy A, editors. Integration of large-scale renewable energy into bulk power systems, pp. VI & 167–185, Power electronics and power systems. Cham: Springer International Publishing; 2017. https://doi.org/10.1007/978-3-319-55581-2.
4 Cochran J, Miller M, Zinaman O, Milligan M, Arent D, Palmintier B, et al. Flexibility in 21st century power systems. 2014. https://doi.org/10.2172/1130630 [United States: N. p., Web].
5 Olauson J, Ayob MN, Bergkvist M, Carpman N, Castellucci V, Goude A, et al. Net load variability in Nordic countries with a highly or fully renewable power system. Nat Energy 2016;1. https://doi.org/10.1038/nenergy.2016.175.
6 Holttinen H. and Hirvonen R., 2005. “Power system requirements for wind power,” in Wind power in power systems, T. Ackermann, Ed. Chichester: Wiley, 2005, pp. 144–167.
7 Hirth L, Ziegenhagen I. Balancing power and variable renewables: three links. Renew Sustain Energy Rev 2015;50:1035–51. https://doi.org/10.1016/j.rser.2015.04.180.
8 Kubik ML, Coker PJ, Barlow JF. Increasing thermal plant flexibility in a high renewables power system. Appl Energy 2015;154:102–11. https://doi.org/10.1016/j.apenergy.2015.04.063.
9 Hong L, Lund H, Möller B. The importance of flexible power plant operation for Jiangsu's wind integration. Energy 2012;41:499–507. https://doi.org/10.1016/j.energy.2012.02.038.
10 Böttger D, Götz M, Lehr N, Kondziella H, Bruckner T. Potential of the power-to-heat technology in district heating grids in Germany. Energy Procedia 2014;46:246–53. https://doi.org/10.1016/j.egypro.2014.01.179.
11 Schweiger G, Rantzer J, Ericsson K, Lauenburg P. The potential of power-to-heat in Swedish district heating systems. Energy 2017;137:661–9. https://doi.org/10.1016/j.energy.2017.02.075.
12 Salpakari J, Mikkola J, Lund PD. Improved flexibility with large-scale variable renewable power in cities through optimal demand side management and power-to-heat conversion. Energ Conver Manage 2016;126:649–61. https://doi.org/10.1016/j.enconman.2016.08.041.
13 Rinne S, Syri S. The possibilities of combined heat and power production balancing large amounts of wind power in Finland. Energy 2015;82:1034–46. https://doi.org/10.1016/j.energy.2015.02.002.
14 Dahl M, Brun A, Andresen GB. Cost sensitivity of optimal sector-coupled district heating production systems. Energy 2019;166:624–36. https://doi.org/10.1016/j.energy.2018.10.044.
15 Dimoulkas I, Amelin M, Levihn F. District heating system operation in power systems with high share of wind power. J Modern Power Syst Clean Energy 2017;5:850–62. https://doi.org/10.1007/s40565-017-0344-6.
16 Lamaison N, Collette S, Vallée M, Bavière R. Storage influence in a combined biomass and power-to-heat district heating production plant. Energy 2019;186:115714. https://doi.org/10.1016/j.energy.2019.07.044.
17 The FENIX vision: The virtual power plant and system integration of distributed energy resources, Contract no: SES6 – 518272, deliverable 1.4.0. Available: http://www.fenix-project.org. [Accessed 3 September 2020] [online].
18 Wille-Haussmann B, Erge T, Wittwer C. Decentralised optimisation of cogeneration in virtual power plants. Solar Energy 2010;84:604–11. https://doi.org/10.1016/j.solener.2009.10.009.
19 Sowa T, Krengel S, Koopmann S, Nowak J. Multi-criteria operation strategies of power-to-heat-systems in virtual power plants with a high penetration of renewable energies. Energy Procedia 2014;46:237–45. https://doi.org/10.1016/j.egypro.2014.01.178.
20 Åberg M, Nilsson AM, Munkhammar J, Luthander R, Lingfors D, Widén J. Electricity self-sufficiency and primary energy use in a Swedish residential community, after building renovation and implementation of photovoltaics, small-scale CHP, and electric vehicles. In: 2016 ACEEE Summer Study on Energy Efficiency in Buildings; 2016.
21 Widén J, Wäckelgård E. A high-resolution stochastic model of domestic activity patterns and electricity demand. Appl Energy 2010;87:1880–92. https://doi.org/10.1016/j.apenergy.2009.11.006.
22 Lingfors D. Solar variability assessment and grid integration. Uppsala University; 2015 [Licentiate thesis, 2015].
23 Frederiksen S, Werner SE. District heating and cooling. 1.th ed. Lund: Studentlitteratur; 2013 [chapter 6.14].
24 Nilsson D. Can biofuels be used to balance variations in electricity production? – a literature study. Report 065. Uppsala: Swedish University of Agricultural Sciences, Department of energy and technology; 2014. p. 2014 [ISSN 1654-9406].
25 Wang J, Zong Y, You S, Træholt C. A review of Danish integrated multi-energy system flexibility options for high wind power penetration. Clean Energy 2017;1:23–35. https://doi.org/10.1093/ce/zkx002.
26 Danish Energy Agency. Flexibility in the power system - Danish and European experiences. Danish Energy Agency; 2015. October 2015.
27 Claesson J, Eftring B, Eskilson P, Hellström G. Markvärme. En handbok om termiska analyser. Del 1 Allmän del (T16:1985). Swedish Built Environment Research Council; 1985, ISBN 91-540-4461-8.
28 SMHI. Uppsalas temperaturserie. URL, SMHI; 2019. https://www.smhi.se/klimatdata/meteorologi/temperatur/uppsalas-temperaturserie-1.2855. [Accessed 15 March 2019] [WWW Document].
29 Nordpool. www.nordpoolgroup.com/historical-market-data/. [Accessed March 2018].
30 Åberg M, Lingfors D, Olauson J, Widén J. Can electricity market prices control power-to-heat production for peak shaving of renewable power generation? The case of Sweden. Energy 2019;176:1–14. https://doi.org/10.1016/j.energy.2019.03.156.
31 Levihn F. CHP and heat pumps to balance renewable power production: lessons from the district heating network in Stockholm. Energy 2017;137:670–8. https://doi.org/10.1016/j.energy.2017.01.118.
32 Lund H, Werner S, Wiltshire R, Svendsen S, Thorsen JE, Hvelplund F, et al. 4th generation district heating (4GDH). Energy 2014;68:1–11. https://doi.org/10.1016/j.energy.2014.02.089.

33 Kostov P. CoordiNet. URL, Innovation and Networks Executive Agency - European Commission; 2019. https://ec.europa.eu/inea/en/horizon-2020/projects/h2020-energy/grids-storage-energy-systems/coordinet. [Accessed 23 August 2020] [WWW Document].
34 Helin K, Zakeri B, Syri S. Is district heating combined heat and power at risk in the Nordic area?—an electricity market perspective. Energies 2018;11:1256. https://doi.org/10.3390/en11051256.
35 Widén J, Carpman N, Castellucci V, Lingfors D, Olauson J, Remouit F, et al. Variability assessment and forecasting of renewables: a review for solar, wind, wave and tidal resources. Renew Sustain Energy Rev 2015;44:356–75. https://doi.org/10.1016/j.rser.2014.12.019.
36 Swedenergy. Power situation in Sweden – reservoir inflow and storage. URL, Swedenergy; 2020. https://www.energiforetagen.se/statistik/kraftlaget/. [Accessed 21 September 2020] [WWW Document, n.d.].
37 SvK. Svenska Kraftnät. Systemutvecklingsplan 2018-2027 – Mot ett flexibelt kraftsystem i en föränderlig omvärld. November 2017. URL, https://www.svk.se/siteassets/om-oss/rapporter/2017/svenska-kraftnats-systemutvecklingsplan-2018-2027.pdf; 2017 [in Swedish, WWW Document, 2017].
38 Länstyrelsen. Förutsättningar för en trygg elförsörjning. URL, https://www.lansstyrelsen.se/skane/tjanster/publikationer/forutsattningar-for-en-trygg-elforsorjning.html. [Accessed 24 September 2020] [in Swedish, WWW Document, n.d.].
39 Suhr M, Klein G, Kourti I, Gonzalo MR, Santonja GG, Roudier S, et al. Best Available Techniques (BAT) reference document for the production of pulp, paper and board 906. LU: Publications Office; 2015. p. 89–90 [2015].
40 Hedström C. Kraftvärmeverk som elnätsreglering för laddfordonsladdning. Uppsala University; 2019 [Master Thesis, February 2019, In Swedish, ISSN: 1650-8300].
41 Hast Aira, Rinne Samuli, Syri Sanna, Kiviluoma Juha, et al. The role of heat storages in facilitating the adaption of district heating systems to large amount of variable renewable electricity. Energy 2017;137:775–88. https://doi.org/10.1016/j.energy.2017.05.113. In this issue.